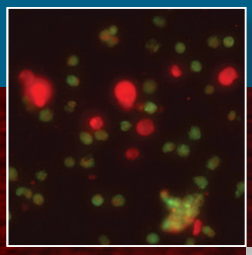

Liquid–liquid phase separation of proteins and peptides derived from biological materials: Discovery, protein engineering, and emerging applications

Yue Sun, Zhi Wei Lim, Qi Guo, Jing Yu, and Ali Miserez

Biological materials represent a major source of inspiration to engineer protein-based polymers that can replicate the properties of living systems. Combined with our ability to control the molecular structure of proteins at the single amino acid level, this results in a vast array of attractive possibilities for materials science, an interest that is undeniably related to simplified procedures in gene synthesis, cloning, and biotechnological production. In parallel, it has been increasingly appreciated that living organisms exploit liquid–liquid phase separation (LLPS) to fabricate extracellular structures. In this article, we discuss the central role of protein LLPS in the fabrication of selected biological structures, including biological adhesives and hard biomolecular composites, and how physicochemical lessons from these systems are being replicated in synthetic analogs. Recent translational applications of protein LLPS are highlighted, notably aqueous-resistant adhesives, stimuli-responsive therapeutics carriers, and matrix materials for green structural composites.

Protein-based biological materials and liquid–liquid phase separation

A central tenet of protein engineering has been to use natural proteins constituting the building blocks of biological tissues as a source of inspiration to produce artificial proteins for various applications. This tradition can be traced back to studies by Weis-Fogh on the elastomeric protein resilin[1] found in the wing hinges of insects. Nowadays, resilin and its derivatives are being extensively developed using protein engineering and investigated as a platform to develop multifunctional protein-based materials.[2,3] With decades of progress in biotechnology processes at our disposal,[4] materials scientists are increasingly benefiting from recombinant protein technology tools to replicate structural proteins for an increasing number of applications.[5–8]

Concurrently, it is increasingly appreciated that the biogenesis of many extracellular biological materials involves liquid–liquid phase separation (LLPS) of their constitutive proteins. LLPS, also called coacervation, occurs from a homogenous solution of biomacromolecules when preferential interactions between constituent molecules disrupt homogeneity, producing coexisting phases: a biopolymer-rich phase usually taking the form of concentrated microdroplets (the coacervates) and a biopolymer-depleted one (**Figure 1**a). In its broad generality, LLPS can be tackled using polymer phase-separation concepts,[9] such as the Flory–Huggins formalism and its unified Overbeek and Voorn extension that incorporates electrostatic interactions. However, proteins encompass a tremendous range of complex features that require advanced multiscale computational modeling in order to describe their phase-separation behavior.[10]

While coacervation has been known for decades in the materials science of soft matter,[11,12] it has witnessed an exciting rejuvenation in the life sciences in the past decade with the realization that LLPS is a widespread phenomenon observed across various length scales of the living world, from the cell

Yue Sun, Nanyang Technological University, Singapore; yue006@e.ntu.edu.sg
Zhi Wei Lim, Nanyang Technological University, Singapore; zwlim@ntu.edu.sg
Qi Guo, Nanyang Technological University, Singapore; guoq0005@e.ntu.edu.sg
Jing Yu, Nanyang Technological University, Singapore; yujing@ntu.edu.sg
Ali Miserez, Nanyang Technological University, Singapore; ali.miserez@ntu.edu.sg
doi:10.1557/mrs.2020.301

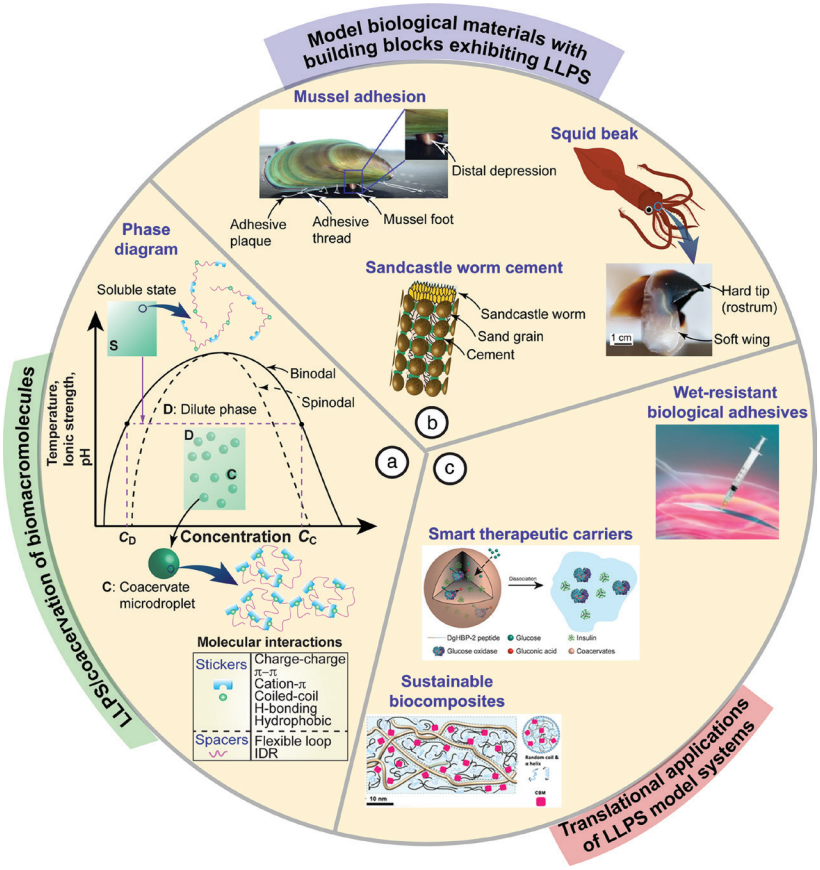

Figure 1. Liquid–liquid phase separation ([LLPS] or coacervation) in biological materials. (a) LLPS can be described by classical binary phase diagrams of polymer solutions. Outside the binodal curve, the system is a homogenous solution. In the region bound by the binodal and the spinodal region, the system is metastable and can rapidly shift between one- and two-phase regimes subject to local fluctuations. Below the spinodal curve, the system is unstable and the solution spontaneously demixes into concentrated coacervate microdroplets (protein/peptide concentration C_c) and a dilute phase (protein/peptide concentration C_D). Biomacromolecules that exhibit LLPS contain multiple "sticker" domains consisting of weak intermolecular attractive interactions, interspersed by flexible linker regions.[9] (b) Protein-based biological materials whose biogenesis involved LLPS include biological adhesives such as the sandcastle worm glue (complex coacervation) and mussel adhesives (self-coacervation), and the squid beak (self-coacervation). (c) Emerging applications exploiting LLPS/coacervation of the natural systems with synthetic proteins and peptides include biological adhesives for soft and hard tissue repair, smart therapeutic carriers, and sustainable biocomposites.[93,101]

nucleus to the extracellular environment.[13,14] LLPS allows for facile, rapid, and dynamic association of disparate biomolecules to facilitate, regulate, and control diverse functions in space and time.[15,16] Coacervate microdroplets display several physicochemical attributes that makes them suitable to enable the processing of extracellular structures. In particular, phase separation occurs under precisely controlled microenvironmental conditions allowing regulation of microdroplet formation and control over the deposition of biopolymers in a spatiotemporal fashion. Furthermore, coacervates exhibit very low interfacial energy[17,18] and a shear-thinning rheological response,[19,20] both of which facilitate the flow of coacervates through porous media during biological materials fabrication.

The importance of coacervation in the processing of extracellular matrix proteins was first recognized in tropoelastin[21]—the precursor of elastin found in a wide range of vertebrate tissues—which phase-separates above a critical temperature close to physiological conditions before self-assembling into elastic fibers. Comprehensive reviews on the coacervation of tropoelastin can be found elsewhere.[14,22,23] Exploiting the LLPS properties of tropoelastin and elastin-like polypeptides (ELPs), myriads of applications have been developed using their synthetic versions, including sustained release of therapeutics,[24] protein purification,[25] or tissue engineering.[26]

We focus this article on protein-based biological structures that have recently been recognized to exhibit LLPS: biological adhesives and protein-based hard tissues (Figure 1b). The primary sequence features driving LLPS are highlighted, followed by a short description of their sequence–structure–property relationships. Emerging bioinspired applications exploiting LLPS are presented, including synthetic wet-resistant adhesives, stimuli-responsive therapeutic carriers, and structural biomolecular composites (Figure 1c).

LLPS/coacervation in biological adhesives

The discovery that LLPS can occur inside the cell[27] has led to an outburst of studies from the life science community in recent years.[28,29] It is perhaps less recognized that LLPS in biological systems was initially proposed to occur in the extracellular environment, as a transient mechanism during which secreted proteins are processed into load-bearing tissues, starting with tropoelastin followed by biological adhesives.[30] Notably, in 2004 Waite and co-workers[31] proposed that the cement proteins secreted by the sandcastle tubeworm to glue together sand particles into a protective tube are assembled by complex coacervation of oppositely charged cement proteins (CPs). The mechanism was later confirmed when the full-length sequences of CPs from the glue were obtained.[32] It was found that CP1 and CP2 are basic proteins with homology to mussel adhesive proteins,[33,34] including the presence of the post-translated amino acid 3,4-dihydroxy-L-phenylalanine (DOPA). A third cement protein, CP3, is highly acidic due to the unusually high abundance of the post-translated amino acid phosphoserine (pSer)

https://doi.org/10.1557/mrs.2020.301

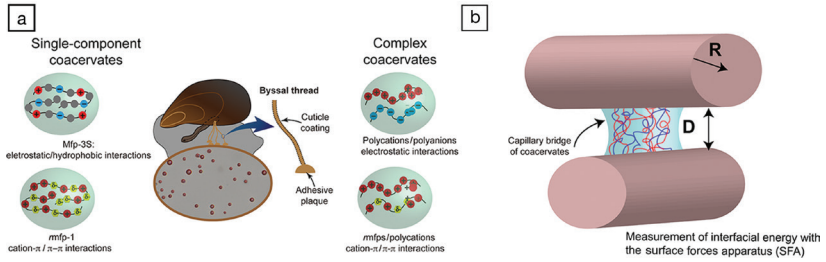

Figure 2. (a) Schematic representation of coacervation of mussel foot proteins (Mfps) and their derived synthetic analogs. Mfp-3S from *Mytulis edulis* species is located in the adhesive plaque, whereas Mfp-1 is the main protein of the protective cuticle. (b) Coacervates can form capillary bridges between two surfaces, and their interfacial energy γ_i can be inferred from the adhesion force required to separate the surfaces. With the surface forces apparatus, the surfaces consist of two cross-cylinders that can measure the contact force *F* and displacement *D* at resolutions of 1 nN and 0.1 nm, respectively.[60] (a) Adapted with permission from Reference 51. © 2018 Royal Society of Chemistry.

that confers a very low isoelectric point below 2.2. Complex coacervation occurs by electrostatic interactions between negatively oppositely charged CPs, with charge balance mediated by divalent Ca^{2+} and Mg^{2+} cations. In the final step, the coacervate microdroplets undergo further phase transitions, first a gelation process quickly followed by curing via side-chain cross-linking between DOPA and cysteine (Cys).[32,35] Complex coacervation offers physicochemical characteristics that are critical for adhesive functionality.[32] The insoluble microdroplets have liquid-like behavior that can flow in seawater but do not disperse, such that a high local concentration of proteins is maintained, which is crucial to obtain a strong adhesive. Furthermore, their low interfacial tension allows the microdroplets to wet sand grains and fill up microscale interstices, providing capillary attractive forces between particles prior to final curing.[30] Exploiting these findings, Stewart and co-workers have produced synthetic polyelectrolyte analogs with polymethacrylate backbones, successfully induced their complex coacervation,[36] and demonstrated their use as biomedical adhesives such as in craniofacial reconstruction.[37] Biomimicry of sandcastle worm complex coacervation has also been achieved with peptidic backbones using a ring-opening polymerization strategy from *N*-carboxyanhydrides (NCAs) precursors, followed by phosphorylation of serine (Ser) residues[38] allowing to obtain pSer/tyrosine co-polypeptides with similar biochemical characteristics as native CP3. Using the same synthesis to obtain Dopa-containing polypeptides mimicking CP-1 and 2,[39] complex coacervates could be achieved by mixing both co-polypeptides.

Mussel adhesive proteins and LLPS

Mussel adhesion has been the archetype model system to fundamentally understand wet adhesion.[34] Mussels sequentially secrete a family of mussel foot proteins (Mfps) with a high content of DOPA[40] that are hierarchically assembled and cured into adhesive filaments (byssal threads). More than 20 different Mfps have been identified and sequenced, initially in the *Mytilus* genus species[34,41] and more recently in species from different geographical locations.[42,43] Wei et al.[44] demonstrated that Mfp-3S could form single-component coacervates stabilized by H-bonding and hydrophobic interactions (**Figure 2**a), and hypothesized that coacervation played a central role to enable secretion in aqueous environments. Recent systematic studies by Harrington and co-workers have indicated that LLPS is critical to the formation of the protecting cuticle surrounding byssal threads.[45,46] To form the cuticle, Mfp-1 (the main protein of the cuticle) and distinct Cys-rich proteins preassemble into distinct fluidic phases within secretory vesicles.[46] Following secretion and deposition, the immiscible fluidic phases are rapidly cured by DOPA-metal coordination bonds, in particular DOPA-Fe and DOPA-Va with distinct bond lifetimes, resulting in a hard, yet extensible coating.[45,47]

Below pH 3.7, both positively charged Mfp-1 or recombinant Mfp-1 (Rmfp-1) with the sequence **M(AKPSYPPTYK)$_{12}$** can form complex coacervates with negatively charged hyaluronic acid (HA) that can protect surfaces against compressive shear forces owing to their lubricant functionality.[48] An alternative design consists in fusing six Mfp-1 decapeptide repeats to both termini of Mfp-5 and Mfp-3 to fabricate hybrid mussel adhesive proteins that are mixed with HA to form complex coacervates.[49,50] Coacervates stabilized by other types of DOPA-mediated interactions, such as hydrogen bonds,[51,52] metal–catechol coordination,[47] and π–π or π–cation interactions[53–57] have also been synthesized using various combinations of Mfps-derived peptides or synthetic polymers.[58] Self-coacervates with strong underwater adhesion have also been achieved by fusing Mfp-5 with a mammalian DNA binding domain exhibiting LLPS.[59] In all these synthetic analogs, synergistic effects combining electrostatic interactions and catechol-mediated interactions all contribute to the strong underwater adhesion of the final product, highlighting the versatility of mussel-inspired coacervates.

Since the interfacial energy γ_i is an important characteristic of coacervates, efforts aimed at accurately measuring this property have been undertaken, in particular with the surface forces apparatus (SFA).[18,44,56] The SFA can measure the capillary adhesion caused by the Laplace pressure across the interface of the coacervate bridge and the aqueous phase (Figure 2b) whereby γ_i is calculated as:[60]

$$\gamma_i = F_{ad}/4\pi R \quad (1)$$

where F_{ad} is the adhesion force measured by the SFA during separation of coacervates bridging two cross-cylinder surfaces, and *R* is their radius of curvature. Using this method, Hwang et al.[18] found that Mfp-1/HA coacervates behave as a

shear-thinning fluid with very low interfacial energy (<1 mJ/m^2). In another study, Priftis and co-workers demonstrated that γ_i of a poly(L-lysine)/poly(L-glutamic acid) coacervate decreases with increasing ionic strength due screening effects.[61] Such measurements are anticipated to be increasingly employed in future work in order to precisely link the molecular structure with interfacial properties.

LLPS in hard biomolecular composites

Squid beak: biomechanics of hard protein-polysaccharide biocomposites

Cephalopods are equipped with a hard beak used by the animal for their hunting and feeding behavior.[62] Owing to its biological function as a hard biotool used for crushing and chewing on prey, studies on *Dosidicus gigas* beak were initiated to assess their mechanical properties,[63] which established that the hard distal part of the beak (called the rostrum) displays a hardness and elastic modulus on par with the hardest thermoset polymers.

Unlike most hard biological mouthparts, the beak is completely uncalcified and only composed of biomacromolecules: the polysaccharide α-chitin and proteins with an overall amino acid composition enriched in glycine (Gly), alanine (Ala) and histidine (His). The closest biological structures to the squid beak are insect exoskeletons (cuticles)[64,65] that also consist of chitin and proteins, many of which are similarly enriched in Gly and tyrosine (Tyr) amino acids as well as His-rich domains.[66] It was subsequently recognized that the beak is a mechanically graded structure that is intimately linked to biomolecular gradients,[67] with cross-linked proteins representing the dominant component of the hard distal rostrum (ca. 70 wt%) whereas the flexible proximal part is mostly made of hydrated chitin. During beak growth, it has been proposed that water is gradually removed from the beak rostrum and substituted by proteins that fill up the porous scaffold. Coacervation has been suggested to be a critical transient step in this process because it would allow proteins to diffuse through the chitin/CBPs networks and to concentrate at the hard region prior to curing. Eventually, beak proteins undergo protein–protein cross-linking, which leads to beak hardening.

Efforts to identify the cross-link chemistry[68] were carried out using tandem mass spectrometry and nuclear magnetic resonance (NMR) measurements on acid hydrolyzed beaks. Cross-links were determined to be His-DOPA side-chain adducts or His covalently cross-linked to low-molecular weight catechols, which is similar to insect cuticle sclerotization.[69] Aromatic cross-linking is well established to dehydrate chitin/protein networks,[70] leading to the notion that strengthening occurs via a synergistic mechanism combining dense covalent cross-linking with chitin dehydration that further enhances the modulus because dry chitin is stiffer than hydrated chitin.

Sequencing and sequence features of squid beak proteins

Having recognized that proteins are the predominant biomolecular components in the hard rostrum begged the question of their primary sequences. However, obtaining the full-length sequence of proteins from highly sclerotized tissues was long considered an intractable task. Because of their highly cross-linked nature, proteins in sclerotized tissues are largely insoluble and only minute amounts can be isolated using even harsh extraction agents, rendering sequencing via traditional proteomic methods exceedingly challenging. Further, genomes are not available for many model organisms of interest. The advent of RNA-sequencing technologies[71] coupled with powerful bioinformatic tools[72] dramatically enhanced our ability to sequence such proteins and led to the discovery of a large number of unknown structural proteins with biomimetic potential. For biological materials, studies first undertaken in our laboratory[42] have relied on an integrative approach combining extraction of mRNA from the epithelial cells[73] where these proteins are expressed followed by the generation of transcriptomic libraries, with high-throughput proteomics[74] of short peptides extracted by chemical cleavage methods.[20] Using this platform, we have obtained full-length sequences not only of the squid beak but of many other structural proteins[42,75–77] that all represent potential model systems to engineer functional proteins. For example, suckerin proteins found in the sucker ring teeth of squids are displaying promising biomedical applications.[78–81]

Two families of proteins have been identified in the squid beak. The first family contains chitin-binding domains that are sought to bind chitin fibrils to form the initial beak scaffold, which is subsequently filled up with the second family of proteins called histidine-rich proteins (HBPs, **Figure 3**a). The N-termini of HBPs are nonrepetitive with domains enriched in Ala, His, and Gly residues. Their C-termini comprise multiple pentapeptide repeats that are rich in Gly, Ala, His, and Tyr. In two of these proteins (HBP-1 and 3), two penta-repeats modules are alternatively arranged with the sequences **GHGXY** or **GHGXH** (module 1), where X is a hydrophobic residue (usually leucine or valine), and **GAGFA** (module 2). HBP-2 only contains multiple copies of module 1. This modular pentapeptide pattern shares homology with the hydrophobic domain of tropoelastin[22] and ELPs that are made of multiple copies of Gly-rich and Pro-rich pentapeptides, prompting us to speculate that HBPs could also coacervate. In contrast to tropoelastin, the repeats motifs of HBPs are rich in His whose pKa is 6.5. Thus, the imidazole group is protonated at weakly acidic pH and it was speculated that LLPS would be pH-dependent. This was corroborated with recombinant HBP-1,[20] which exhibited not only pH-dependent LLPS, but also shear-thinning rheological properties of the dense phase.

Squid beak proteins as model systems of LLPS investigations

By exploiting the low sequence complexity of the repetitive domains of HBPs, truncated peptide (HBP-*peps*) constructs made of diverse copies of modules 1 and 2 offer opportunities to dissect out the molecular mechanisms of LLPS and to connect biophysical properties of microdroplets with their

https://doi.org/10.1557/mrs.2020.301

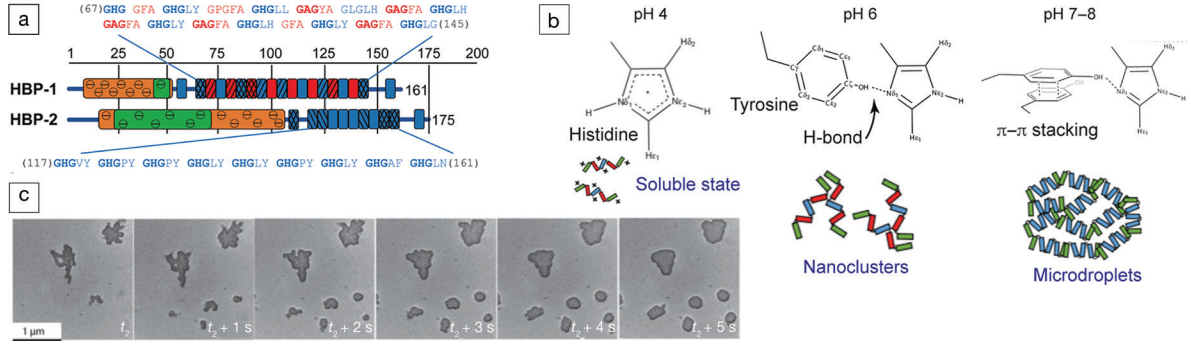

Figure 3. (a) The squid beak is made of chitin, chitin-binding proteins, and histidine-rich beak proteins (HBPs). The C-termini of HBPs are tandem repeats of pentapeptides (sequences shown on top).[82] (b) HBPs and HBP-*peps* display pH-responsive liquid–liquid phase separation governed by deprotonation of His amino acid. His residues are positively charged below pH 6.5, resulting in repulsive interactions that maintain HPBs and HPP-*peps* in solution. Nuclear magnetic resonance investigations have shown that upon pH increase, His form transient hydrogen bonds with Tyr residues, resulting in nanoclusters that further grow into microdroplets stabilized through π–π interactions of Tyr side chains.[83] (c) Nanocluster nucleation and growth into microdroplets can be dynamically captured by liquid-phase transmission electron microscopy without using any contrasting agents, as exemplified here for the growth of HBP-2 nanoclusters.[90]

molecular structure. For example, there is a strong interest to link the visco-elastic properties of microdroplets with their amino acid sequence features.[28] Using 23–26 amino acid long peptides constructed with module 1 and module 2 repeats, Cai et al.[82] demonstrated that the substitution of two modules 1 (**GHGXY/H**) with the more hydrophobic module 2 (**GAGFA**) led to a two order of magnitude increase in storage modulus G' as well as to a transition from liquid-like to a viscous gel rheological response, indicating that the visco-elasticity of microdroplets can be tuned by relatively simple amino acid mutations. In another recent study, Gabryelczyk et al.[83] employed double- and triple-resonance nuclear magnetic resonance (NMR) spectroscopy and verified that HBP-1 is an intrinsically disordered protein (IDP), a common characteristic of many proteins exhibiting LLPS.[84] Tandem repeat peptides with various numbers of modules 1 and 2 were also systematically explored, and the **GHGLY** repeat was identified as essential to induce LLPS. Usually at least two copies of this motif were required to induce LLPS, which should be separated by spacers about 15 amino acid long. Mutating the Tyr residue in position five of the pentapeptide for Ala abolished phase separation, pointing out to the critical role of aromatic Tyr. Further investigations with two-dimensional solution NMR and multidimensional solid-state NMR revealed that pH-activated LLPS in these peptides occurs via a multistep oligomerization cascade, illustrated in Figure 3b. As the pH increases, deprotonation of His residues triggers the creation of transient H-bonds between the imidazole group of His and the aromatic ring of Tyr, thereby nucleating oligomeric units. Subsequently, π–π stacking between Tyr residues stabilize the coacervate microdroplets. More generally speaking, these studies highlight that solution and solid-state NMR spectroscopy techniques are ideally suited to reveal intricate details on the dynamic molecular events driving LLPS. Accordingly, an increasing number of LLPS systems are currently being investigated with protein NMR methods.[85–87]

Because of the intrinsic dynamic properties of proteins involved in LLPS, new tools that can probe these systems with spatial and time resolution are needed.[29,88] For example, the nucleation and growth steps of nanoclusters that eventually develop into microdroplets are still not well understood.[9,28] Recent advances in transmission electron microscopy (TEM) enable to observe organic matter in liquid without contrasting agents, in principle allowing to observe dynamic assembly during LLPS.[89] Using this technique, Le Ferrand et al.[90] were able to capture nucleation and growth kinetics of nanoclusters of HBP-2 with millisecond time resolution and to quantitatively assess the role of variables such as ionic strength on the kinetics of nanocluster formation (Figure 3c). Since *in situ* liquid TEM allows direct observation without staining agents that may disrupt the phase separation behavior, this tool is anticipated to provide important insights into nucleation and growth phenomena of LLPS at the nanoscale.

Emerging applications of squid beak derived peptide in smart drug delivery

The realization that HBPs tandem repeat regions share some similarity with ELPs have prompted investigations in unexpected areas such as encapsulation of therapeutics with stimuli-responsive delivery. These studies were stimulated by two main features. First, given the ability of coacervates to encapsulate a wide range of both low molecular weight compounds and macromolecules,[91,92] it was postulated that client molecules could be recruited within HBP-*peps* droplets. Second, the high abundance of His should allow to manipulate the pH-responsive phase separation of HBP-*peps* around physiological pH, with coacervation occurring at neutral pH and disassembly into a single phase at weakly acidic pH, in turn allowing recruited cargos to be released by lowering the pH. Accordingly, Lim et al.[93] designed the peptide HBP-*pep2* and created a coacervate-based glucose/pH responsive insulin delivery system

https://doi.org/10.1557/mrs.2020.301

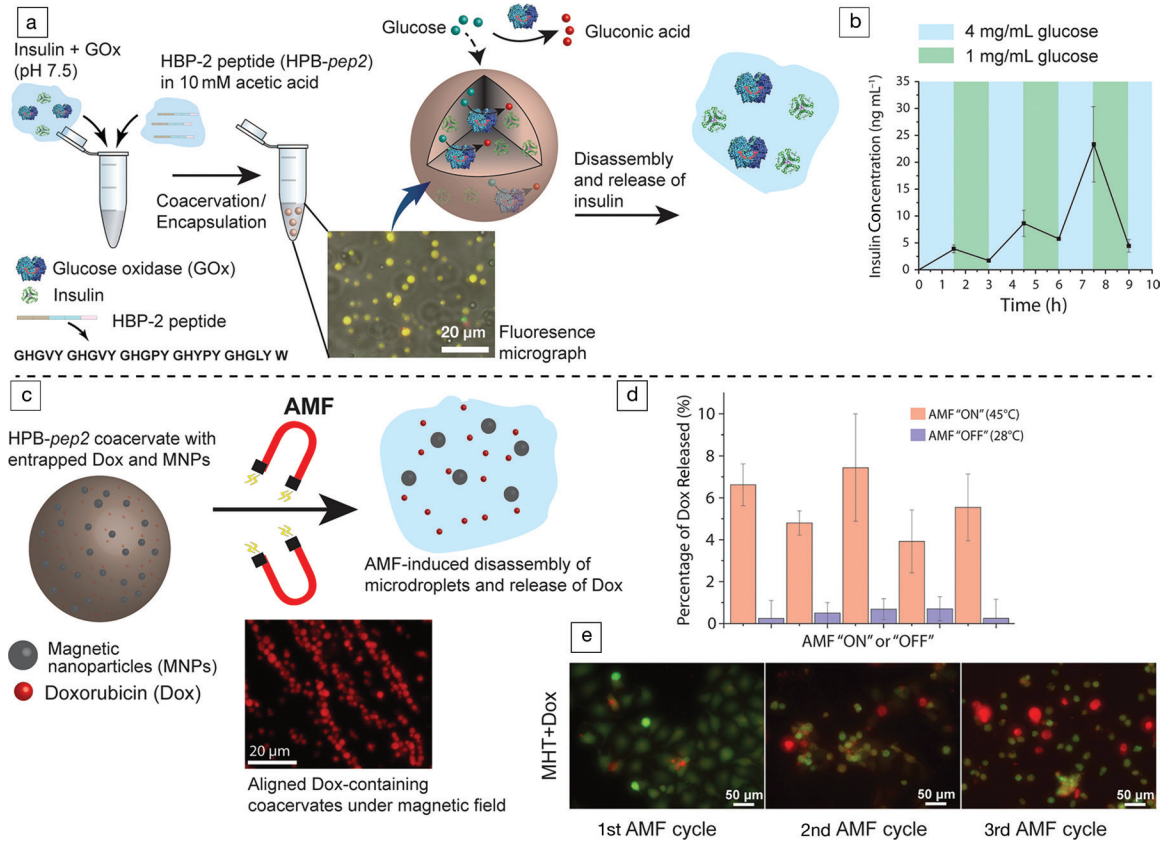

Figure 4. Histidine-rich beak protein (HBP)-*pep2* coacervates for therapeutic encapsulation and smart release. (a) Encapsulation of insulin and GOx into HBP-*pep2* coacervates, which occurs nearly instantaneously upon mixing HBP-*pep2* in the insulin + GOx solution. Yellow droplets in the fluorescence micrograph indicate co-localization of insulin and GOx. At hyperglycemic conditions, glucose diffuse into the coacervates and is converted into gluconic acid by GOx. Buildup of gluconic acid results in an acidic microenvironment that triggers disassembly of coacervates and release of insulin. (b) The *in vitro* release of insulin from the coacervates is modulated depending on high (blue) and low (green) glucose concentration. (c) HBP-*pep2* coacervates can also co-recruit magnetic nanoparticles (MNPs) and doxorubicin (Dox). Red droplets are aligned in bead-like chains when applying a magnetic field, indicating magnetic responsiveness. Upon application of an alternating magnetic field (AMF), the microdroplets are locally heated via magnetic hyperthermia (MHT), resulting in disassembly and release of Dox. (d) The rate of Dox release can be modulated by turning AMF "on" and "off." (e) After three cycles of AMF, 100% nearly *in vitro* cell death is achieved in HepG2 liver cancer cells. (a, b) Adapted with permission from Reference 93. © 2018 American Chemical Society. (c–e) Reprinted with permission from Reference 95. © Elsevier 2020.

(GRIDS) loaded with insulin and glucose oxidase (GOx) (with a recruitment efficiency of insulin above 99%), which acted as a glucose sensor (**Figure 4**a). At hyperglycemic conditions, glucose diffused into the GRIDS and was converted into gluconic acid by GOx, resulting in an acidic microenvironment that ultimately triggered the disassembly and the release of insulin from the microdroplets. The release kinetics of insulin was reversible and dependent on the glucose levels (Figure 4b). The secondary structure of released insulin was not affected, suggesting that it retained its bioactivity in agreement with previous reports demonstrating that coacervation is a gentle encapsulation method that enhances the stability of cargo molecules.[91,94]

HBP-*pep2* coacervates are also able to recruit small-molecule drugs and inorganic nanoparticles,[95] which can be used to co-encapsulate doxorubicin (Dox) and magnetic nanoparticles (MNPs) for thermo-chemotherapy of liver cancer cells (Figure 4c). The incorporation of MNPs within the Dox delivery system gave rise to magnetic targeting and magnetic hyperthermia (MHT)-controlled Dox release, which could be controlled by inducing heating via the application of an external alternating magnetic field (AMF), resulting in a MHT effect that can disassemble the coacervates and release Dox (Figure 4d). Critically, the microdroplets readily crossed the cell membrane and the release of the Dox cargo could occur intracellularly, although it did not follow classical endocytosis of cellular internalization. MHT enhanced the cytotoxic effect of Dox such that the thermo-chemotherapy (MHT + Dox) treatment on HepG2 liver cancer cells resulted in 100% cell death (Figure 4e). While the mechanism of cellular uptake is still unknown, the ability of HBP-*pep2* coacervates to cross the cell membrane offers exciting opportunities for intracellular delivery of macromolecular therapeutics, which remains a major challenge.[96]

https://doi.org/10.1557/mrs.2020.301

Protein engineering of silk-reinforced proteins with LLPS ability

Given their strong mechanical properties, spider silk proteins (spidroins) have been an obvious target of protein engineering efforts for materials applications, and their production through recombinant technologies has been ongoing since the mid-1990s.[7,97] One issue faced has been the insoluble nature of recombinant spidroins, which often aggregate in the inclusion body and require harsh solvents for their purification, although important progress have recently been achieved to overcome this issue.[98] Another strategy developed by Linder and coworkers has been to produce spidroin-based multifunctional recombinant proteins with LLPS ability, as a way to facilitate their subsequent self-assembly into mechanically robust structures. Thus, Mohammadi et al.[99] designed a three-block architecture fusion protein consisting of a central, repetitive spidroin domain flanked by globular cellulose binding module (CBM) domains (Figure 1c). They found that the three-block architecture formed coacervates, from which a few µ1 droplets could be drawn into macroscopic fibers with an elastic-plastic tensile response. LLPS was critical because it provided an intermediate step during which the proteins are concentrated before the final assembly into solid fibers.

This protein engineering platform was subsequently deployed for various load-bearing applications. For example, owing to the presence of the CBM domain, the coacervates were used as strong adhesives to various cellulose-based substrates.[100] This group also used their three-block spidroin/CBM coacervates to create protein/cellulose nanofibril (CNF) nanocomposites,[101] with the protein coacervate playing the role of the matrix and CNF that of the reinforcing phase. CBM domains greatly enhanced the mechanical properties of the composites by forming strong molecular-level binding interfaces with CNF, thereby promoting efficient load transfer from the protein matrix to the reinforcing nanocellulose fibrils. Without the CMB domain, or if the three-block protein was not pre-processed into coacervates, there were weaker molecular interfaces that resulted in premature failure. Such studies are promising because they offer interesting opportunities to produce eco-friendly "bioplastic" composites that could represent one avenue to mitigate the enormous challenge of petro-derived polymers and their unsustainable accumulation in landfills and marine ecosystems.[102]

Outlook

Multifunctional protein materials are attractive because of our ability to precisely tune their physicochemical and mechanical properties. Concurrently, the realization that LLPS represents a broad biological strategy has expanded the potential of protein-based materials. The control of LLPS via protein engineering strategies holds promise for biological adhesives and the development of multifunctional, stimuli-responsive drug carriers. Another emerging area is eco-friendly and mechanically robust biocomposites, which could represent sustainable materials free of fossil-fuel derived feedstock. However, there are challenges ahead before their potential can be fulfilled, notably to improve expression yield and reduce cost of production, although there are recent encouraging developments addressing this issue.

We also hope to highlight the need to pursue fundamental studies of biological systems. All of the model systems presented here, from mussel adhesives to the sandcastle worm glue to the squid beak were initiated by curiosity-driven explorations without an obvious target application in mind. Identification of their full-length sequences and the realization that they exhibit LLPS are now being exploited in unforeseen applications.

Acknowledgments

A.M. acknowledges financial support from the Singapore Ministry of Education (Grant Nos. MOE 2018-T2–1-043 and MOE 2019-T3-1-012) and from the Strategic Initiative on Biomimetic and Sustainable Materials (IBSM) at NTU. J.Y. acknowledges financial support from the Singapore National Research Foundation Fellowship (NRF-NRFF11–2019-0004).

References

1. T. Weis-Fogh, *J. Exp. Biol.* **37**, 889 (1960).
2. C.M. Elvin, A.G. Carr, M.G. Huson, J.M. Maxwell, R.D. Pearson, T. Vuocolo, N.E. Liyou, D.C.C. Wong, D.J. Merritt, N.E. Dixon, *Nature* **437**, 999 (2005).
3. L. Li, T. Luo, K.L. Kiick, *Macromol. Rapid Commun.* **36**, 90 (2015).
4. T.A. Brown, *Gene Cloning and DNA Analysis: An Introduction*, 6th ed. (Wiley, Hoboken, NJ, 2016).
5. O. Tokareva, V.A. Michalczechen-Lacerda, E.L. Rech, D.L. Kaplan, *Microb. Biotechnol.* **6**, 651 (2013).
6. G.C. Yeo, B. Aghaei-Ghareh-Bolagh, E.P. Brackenreg, M.A. Hiob, P. Lee, A.S. Weiss, *Adv. Healthc. Mater.* **4**, 2530 (2015).
7. A. Heidebrecht, T. Scheibel, in *Advances in Applied Microbiology*, S. Sariaslani, G.M. Gadd, Eds. (Academic Press, Cambridge, MA, 2013), vol. 82, pp. 115–153.
8. Y.J. Yang, A.L. Holmberg, B.D. Olsen, *Annu. Rev. Chem. Biomol. Eng.* **8**, 549 (2017).
9. C.P. Brangwynne, P. Tompa, R.V. Pappu, *Nat. Phys.* **11**, 899 (2015).
10. G.L. Dignon, W. Zheng, J. Mittal, *Curr. Opin. Chem. Eng.* **23**, 92 (2019).
11. H.G. Bungenberg de Jong, H.R. Kruyt, in *Colloid Science*, H.R. Kruyt, Ed. (Elsevier, Amsterdam, The Netherlands, 1949), vol. 2, pp. 433–482.
12. C.L. Cooper P.L. Dubin, A.B. Kayitmazer, S. Turksen, *Curr. Opin. Colloid Interface Sci.* **10**, 52 (2005).
13. Y. Shin, C.P. Brangwynne, *Science* **357**, eaaf4382 (2017).
14. L.D. Muiznieks, S. Sharpe, R. Pomès, F.W. Keeley, *J. Mol. Biol.* **430**, 4741 (2018).
15. S. Boeynaems, S. Alberti, N.L. Fawzi, T. Mittag, M. Polymenidou, F. Rousseau, J. Schymkowitz, J. Shorter, B. Wolozin, L. Van Den Bosch, P. Tompa, M. Fuxreiter, *Trends Cell Biol.* **28**, 420 (2018).
16. S. Alberti, *Curr. Biol.* **27**, R1097 (2017).
17. E. Spruijt, J. Sprakel, M.A. Cohen Stuart, J. van der Gucht, *Soft Matter* **6**, 172 (2009).
18. D.S. Hwang, H. Zeng, A. Srivastava, D.V. Krogstad, M. Tirrell, J.N. Israelachvili, J.H. Waite, *Soft Matter* **6**, 3232 (2010).
19. E. Kizilay, A.B. Kayitmazer, P.L. Dubin, *Adv. Colloid Interface Sci.* **167**, 24 (2011).
20. Y.P. Tan, S. Hoon, P.A. Guerette, W. Wei, C. Hao, A. Ghadban, A. Miserez, J.H. Waite, *Nat. Chem. Biol.* **11**, 488 (2015).
21. D.W. Urry, *J. Protein Chem.* **7**, 1 (1988).
22. G.C. Yeo, F.W. Keeley, A.S. Weiss, *Adv. Colloid Interface Sci.* **167**, 94 (2011).
23. S.G. Wise, G.C. Yeo, M.A. Hiob, J. Rnjak-Kovacina, D.L. Kaplan, M.K.C. Ng, A.S. Weiss, *Acta Biomater.* **10**, 1532 (2014).
24. K.M. Luginbuhl, J.L. Schaal, B. Umstead, E.M. Mastria, X. Li, S. Banskota, S. Arnold, M. Feinglos, D. D'Alessio, A. Chilkoti, *Nat. Biomed. Eng.* **1**, 0078 (2017).
25. D.E. Meyer, A. Chilkoti, *Nat. Biotechnol.* **17**, 1112 (1999).
26. S. Roberts, T.S. Harmon, J.L. Schaal, V. Miao, K. Li, A. Hunt, Y. Wen, T.G. Oas, J.H. Collier, R.V. Pappu, A. Chilkoti, *Nat. Mater.* **17**, 1154 (2018).
27. C.P. Brangwynne, C.R. Eckmann, D.S. Courson, A. Rybarska, C. Hoege, J. Gharakhani, F. Jülicher, A.A. Hyman, *Science* **324**, 1729 (2009).
28. S. Alberti, A. Gladfelter, T. Mittag, *Cell* **176**, 419 (2019).

29. D. Bracha, M.T. Walls, C.P. Brangwynne, *Nat. Biotechnol.* **37**, 1435 (2019).
30. R.J. Stewart, C.S. Wang, I.T. Song, J.P. Jones, *Adv. Colloid Interface Sci.* **239**, 88 (2017).
31. R.J. Stewart, J.C. Weaver, D.E. Morse, J.H. Waite, *J. Exp. Biol.* **207**, 4727 (2004).
32. H. Zhao, C. Sun, R.J. Stewart, J.H. Waite, *J. Biol. Chem.* **280**, 42938 (2005).
33. J.H. Waite, R.A. Jensen, D.E. Morse, *Biochemistry* **31**, 5733 (1992).
34. J.H. Waite, *J. Exp. Biol.* **220**, 517 (2017).
35. C.S. Wang, R.J. Stewart, *Biomacromolecules* **14**, 1607 (2013).
36. R.J. Stewart, C.S. Wang, H. Shao, *Adv. Colloid Interface Sci.* **167**, 85 (2011).
37. B.D. Winslow, H. Shao, R.J. Stewart, P.A. Tresco, *Biomaterials*, **31**, 9373 (2010).
38. V. Lipik, L. Zhang, A. Miserez, *Polym. Chem.* **5**, 1351 (2014).
39. L. Zhang, V. Lipik, A. Miserez, *J. Mater. Chem. B* **4**, 1544 (2016).
40. P.L. Lee, P.B. Messersmith, J.N. Israelachvili, J.H. Waite, *Annu. Rev. Mater. Res.* **41**, 99 (2011).
41. M.J. Harrington, J.H. Waite, *J. Exp. Biol.* **210**, 4307 (2007).
42. P.A. Guerette, S. Hoon, Y. Seow, F.T. Wong, V.H.B. Ho, M. Raida, A. Masic, M.C. Demirel, F. Abdon, S. Amini, G.Z. Tay, D. Ding, A. Miserez, *Nat. Biotechnol.* **31**, 908 (2013).
43. A. Gantayet, D.J. Rees, E.D. Sone, *Mar. Biotechnol.* **16**, 144 (2014).
44. W. Wei, Y. Tan, N.R.M. Rodriguez, J. Yu, J.N. Israelachvili, J.H. Waite, *Acta Biomater.* **10**, 1663 (2014).
45. F. Jehle, E. Macías-Sánchez, S. Sviben, P. Fratzl, L. Bertinetti, M.J. Harrington, *Nat. Commun.* **11**, 862 (2020).
46. T. Priemel, E. Degtyar, M.N. Dean, M.J. Harrington, *Nat. Commun.* **8**, 14539 (2017).
47. M.J. Harrington, A. Masic, N. Holten-Andersen, J.H. Waite, P. Fratzl, *Science* **328**, 216 (2010).
48. D.R. Miller, S. Das, K.-Y. Huang, S. Han, J.N. Israelachvili, J.H. Waite, *ACS Biomater. Sci. Eng.* **1**, 1121 (2015).
49. D.S. Hwang, Y. Gim, H.J. Yoo, H.J. Cha, *Biomaterials* **28**, 3560 (2007).
50. S. Lim, Y.S. Choi, D.G. Kang, Y.H. Song, H.J. Cha, *Biomaterials* **31**, 3715 (2010).
51. Q. Guo, J. Chen, J. Wang, H. Zeng, J. Yu, *Nanoscale* **12**, 1307 (2020).
52. J. Yu, W. Wei, M.S. Menyo, A. Masic, J.H. Waite, J.N. Israelachvili, *Biomacromolecules* **14**, 1072 (2013).
53. D.S. Hwang, H. Zeng, Q. Lu, J. Israelachvili, J.H. Waite, *Soft Matter* **8**, 5640 (2012).
54. Q. Lu, D.X. Oh, Y. Lee, Y. Jho, D.S. Hwang, H. Zeng, *Angew. Chem. Int. Ed.* **52**, 3944 (2013).
55. S. Park, S. Kim, Y. Jho, D.S. Hwang, *Langmuir* **35**, 16002 (2019).
56. S. Kim, J. Huang, Y. Lee, S. Dutta, H.Y. Yoo, Y.M. Jung, Y. Jho, H. Zeng, D.S. Hwang, *Proc. Natl. Acad. Sci. U.S.A.* **113**, E847 (2016).
57. S. Seo, S. Das, P.J. Zalicki, R. Mirshafian, C.D. Eisenbach, J.N. Israelachvili, J.H. Waite, B.K. Ahn, *J. Am. Chem. Soc.* **137**, 9214 (2015).
58. Q. Zhao, D.W. Lee, B.K. Ahn, S. Seo, Y. Kaufman, J.N. Israelachvili, J.H. Waite, *Nat. Mater.* **15**, 407 (2016).
59. M. Cui, X. Wang, B. An, C. Zhang, X. Gui, K. Li, Y. Li, P. Ge, J. Zhang, C. Liu, C. Zhong, *Sci. Adv.* **5**, eaax3155 (2019).
60. J.N. Israelachvili, *Intermolecular and Surface Forces*, 3rd ed. (Academic Press, Cambridge MA, USA, 2011).
61. D. Priftis, R. Farina, M. Tirrell, *Langmuir* **28**, 8721 (2012).
62. M.R. Clarke, Ed., *A Handbook for the Identification of Cephalopod Beaks* (Clarendon Press, Oxford, UK, 1986).
63. A. Miserez, Y. Li, J.H. Waite, F. Zok, *Acta Biomater.* **3**, 139 (2007).
64. S.A. Andersen, P. Hojrup, P. Roepstorff, *Insect Biochem. Mol. Biol.* **25**, 153 (1995).
65. D. Rubin, A. Miserez, J.H. Waite, in *Advances in Insect Physiology*, J. Casas, Ed. (Elsevier, Amsterdam, The Netherlands, 2010), vol. 38, pp. 75–133.
66. J.H. Willis, V.A. Iconomidou, V.F. Smith, S. Hamodrakas, in *Comprehensive Molecular Insect Science*, L. Gilbert, K. Iatrou, S. Gill, Eds. (Elsevier, Oxford, UK, 2005), vol. 4, pp. 79–110.
67. A. Miserez, T. Schneberk, C. Sun, F. W. Zok, J.H. Waite, *Science* **319**, 1816 (2008).
68. A. Miserez, D. Rubin, J.H. Waite, *J. Biol. Chem.* **285**, 38115 (2010).
69. J. Schaefer, K. Kramer, J. Garbow, G. Jacob, E. Stejskal, T. Hopkins, R. Speirs, *Science* **235**, 1200 (1987).
70. S.A. Andersen, *Insect Biochem. Mol. Biol.* **40**, 166 (2010).
71. F. Ozsolak, P.M. Milos, *Nat. Rev. Genet.* **12**, 87 (2011).
72. M.G. Grabherr, B.J. Haas, M. Yassour, J.Z. Levin, D.A. Thompson, I. Amit, X. Adiconis, L. Fan, R. Raychowdhury, Q. Zeng, Z. Chen, E. Mauceli, N. Hacohen, A. Gnirke, N. Rhind, F. Di Palma, B.W. Birren, C. Nusbaum, K. Lindblad-Toh, N. Friedman, A. Regev, *Nat. Biotechnol.* **29**, 644 (2011).
73. P.N. Dilly, M. Nixon, *Cell Tissue Res.* **167**, 229 (1976).
74. B. Ma, K. Zhang, C. Hendrie, C. Liang, M. Li, A. Doherty-Kirby, G. Lajoie, *Rapid Commun. Mass Spectrom.* **17**, 2337 (2003).
75. P.A. Guerette, S. Hoon, D. Ding, S. Amini, A. Masic, B. Venkatesh, V. Ravi, J.C. Weaver, A. Miserez, *ACS Nano* **8**, 7170 (2014).
76. J.J. Loke, A. Kumar, S. Hoon, C. Verma, A. Miserez, *Biomacromolecules* **18**, 931 (2017).
77. S. Amini, M. Tadayon, J.J. Loke, A. Kumar, D. Kanagavel, H. Le Ferrand, M. Duchamp, M. Raida, R.M. Sobota, L. Chen, S. Hoon, A. Miserez, *Proc. Natl. Acad. Sci. U.S.A.* **116**, 8685 (2019).
78. Y. Ping, D. Ding, R.A.N.S. Ramos, H. Mohanram, K. Deepankumar, J. Gao, G. Tang, A. Miserez, *ACS Nano* **11**, 4528 (2017).
79. S.H. Hiew, A. Miserez, *ACS Biomater. Sci. Eng.* **3**, 680 (2017).
80. D. Ding, J. Pan, S.H. Lim, S. Amini, L. Kang, A. Miserez, *J. Mater. Chem. B* **5**, 8467 (2017).
81. K. Deepankumar, C. Lim, I. Polte, B. Zappone, C. Labate, M.P. De Santo, H. Mohanram, A. Palaniappan, D.S. Hwang, A. Miserez, *Adv. Funct. Mater.* **30**, 1907534 (2020).
82. H. Cai, B. Gabryelczyk, M.S.S. Manimekalai, G. Grüber, S. Salentinig, A. Miserez, *Soft Matter* **13**, 7740 (2017).
83. B. Gabryelczyk, H. Cai, X. Shi, S. Yue, P.J.M. Swinkels, S. Salentinig, K. Pervushin, A. Miserez, *Nat. Commun.* **10**, 5465 (2019).
84. V.N. Uversky, *Adv. Colloid Interface Sci.* **239**, 97 (2017).
85. J.P. Brady, P.J. Farber, A. Sekhar, Y.-H. Lin, R. Huang, A. Bah, T.J. Nott, H.S. Chan, A.J. Baldwin, J.D. Forman-Kay, L.E. Kay, *Proc. Natl. Acad. Sci. U.S.A.* **114**, E8194 (2017).
86. S.E. Reichheld, L.D. Muiznieks, F.W. Keeley, S. Sharpe, *Proc. Natl. Acad. Sci. U.S.A.* **114**, E4408 (2017).
87. D.T. Murray, M. Kato, Y. Lin, K.R. Thurber, I. Hung, S.L. McKnight, R. Tycko, *Cell* **171**, 615 (2017).
88. A. Lampel, *Chem* **6**, 1222 (2020).
89. J.J. De Yoreo, N.A.J.M. Sommerdijk, *Nat. Rev. Mater.* **1**, 16035 (2016).
90. H. Le Ferrand, M. Duchamp, B. Gabryelczyk, H. Cai, A. Miserez, *J. Am. Chem. Soc.* **141**, 7202 (2019).
91. K.A. Black, D. Priftis, S.L. Perry, J. Yip, W.Y. Byun, M. Tirrell, *ACS Macro Lett.* **3**, 1088 (2014).
92. N.R. Johnson, M. Kruger, K.P. Goetsch, P. Zilla, D. Bezuidenhout, Y. Wang, N.H. Davies, *ACS Biomater. Sci. Eng.* **1**, 753 (2015).
93. Z.W. Lim, Y. Ping, A. Miserez, *Bioconjug. Chem.* **29**, 2176 (2018).
94. D. Priftis, L. Leon, Z. Song, S.L. Perry, K.O. Margossian, A. Tropnikova, J. Cheng, M. Tirrell, *Angew. Chem. Int. Ed.* **54**, 11128 (2015).
95. Z.W. Lim, V. Varma, R.V. Ramanujan, A. Miserez, *Acta Biomater.* **110**, 221 (2020).
96. S. Du, S.S. Liew, L. Li, S.Q. Yao, *J. Am. Chem. Soc.* **140**, 15986 (2018).
97. X.X. Xia, Z.G. Qian, C.S. Ki, Y.H. Park, D.L. Kaplan, S.Y. Lee, *Proc. Natl. Acad. Sci. U.S.A.* **107**, 14059 (2010).
98. M. Andersson, Q. Jia, A. Abella, X.-Y. Lee, M. Landreh, P. Purhonen, H. Hebert, M. Tenje, C.V. Robinson, Q. Meng, G.R. Plaza, J. Johansson, A. Rising, *Nat. Chem. Biol.* **13**, 262 (2017).
99. P. Mohammadi, A.S. Aranko, L. Lemetti, Z. Cenev, Q. Zhou, S. Virtanen, C.P. Landowski, M. Penttilä, W.J. Fischer, W. Wagermaier, M.B. Linder, *Commun. Biol.* **1**, 86 (2018).
100. P. Mohammadi, G. Beaune, B.T. Stokke, J.V.I. Timonen, M.B. Linder, *ACS Macro Lett.* **7**, 1120 (2018).
101. P. Mohammadi, A.S. Aranko, C.P. Landowski, O. Ikkala, K. Jaudzems, W. Wagermaier, M.B. Linder, *Sci. Adv.* **5**, eaaw2541 (2019).
102. R. Geyer, J.R. Jambeck, K.L. Law, *Sci. Adv.* **3**, e1700782 (2017). □

Yue Sun has been a doctoral candidate at Nanyang Technological University, Singapore, since 2018. He received his bachelor's and master's degrees in materials science and engineering from Beijing University of Chemical Technology, China, in 2014 and 2017, respectively. His research interests include biomimetic materials, polymer chemistry, biomaterials characterization, and drug delivery. His current research focuses on liquid–liquid phase separation of squid beak proteins and peptides, and their potential applications in biomedicine. Sun can be reached by email at yue006@e.ntu.edu.sg.

https://doi.org/10.1557/mrs.2020.301

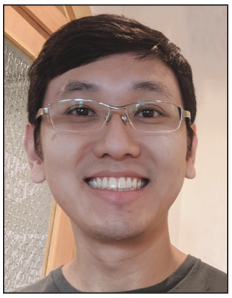

Zhi Wei Lim is a postdoctoral researcher in the School of Materials Science and Engineering at Nanyang Technological University (NTU), Singapore. He received both his PhD degree in materials science and engineering and BSc degree in biological sciences from NTU. He was a research officer at the Institute of Molecular and Cell Biology in the Agency for Science, Technology and Research, Singapore, until 2016. His research interests include coacervate-based drug delivery systems and genetic manipulation. Lim can be reached by email at zwlim@ntu.edu.sg.

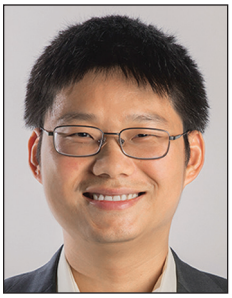

Jing Yu is an assistant professor in the School of Materials Science and Engineering at Nanyang Technological University, Singapore. He obtained his PhD degree in chemical engineering from the University of California, Santa Barbara, in 2012. He completed postdoctoral research at The University of Chicago. The goal of his research is to characterize dynamic properties of interfaces with hierarchical structures and to gain molecular-level control of soft interfaces to enable the design of integrated, multifunctional interfaces. Yu can be reached by email at yujing@ntu.edu.sg.

Qi Guo is a doctoral candidate of materials science and engineering at Nanyang Technological University, Singapore. She received her BSc degree in chemistry from Fudan University, China, in 2018. Her current research focuses on marine-inspired adhesive proteins and peptides. Qi can be reached by email at guoq0005@e.ntu.edu.sg.

Ali Miserez has been a faculty member at Nanyang Technological University, Singapore, since 2009. He received his PhD degree from École Polytechnique Fédérale de Lausanne, Switzerland, in 2003. He completed postdoctoral research at the University of California, Santa Barbara. In 2011, he was awarded the Singapore NRF Fellowship, a $3 million individual grant for early-career scientists. His current research focuses on revealing the molecular, physicochemical, and structural principles from biological materials, and translating these discoveries into novel biomimetic materials. Miserez can be reached by email at ali.miserez@ntu.edu.sg.

https://doi.org/10.1557/mrs.2020.301